Supplementary material (ESI) for Soft Matter

Electronic Supplementary Information

Wetting and friction on superoleophobic surfaces

Laurent Joly and Thierry Biben
Université de Lyon, F-69000, Lyon, France; Université Lyon 1, F-69622, Villeurbanne, France; CNRS, UMR5586, Laboratoire PMCN.

A Finite element modeling

In order to quantify the influence of geometry and contact angle on the slip properties of SO surfaces at reasonable computational cost, we turned to finite element calculations. We modeled a newtonian liquid in the Stokes regime confined between a smooth wall and a SO surface, in the fakir state, as illustrated in Fig 5.c. For the sake of simplicity, we imposed a perfect-slip BC (zero friction) at the liquid/vapor interface, and a no-slip BC at the liquid/solid interface. These assumptions can easily be lifted, introducing finite slip BC with different slip lengths on the vapor and solid surfaces, but this does not modify qualitatively our conclusions. Every dimension was normalized with the pattern periodicity L. We used a distance between the two walls large enough so that the results do not depend on it (typically 1.5). The effective hydrodynamic BC on the SO surface was probed by imposing a Couette flow and a Poiseuille flow in the system.

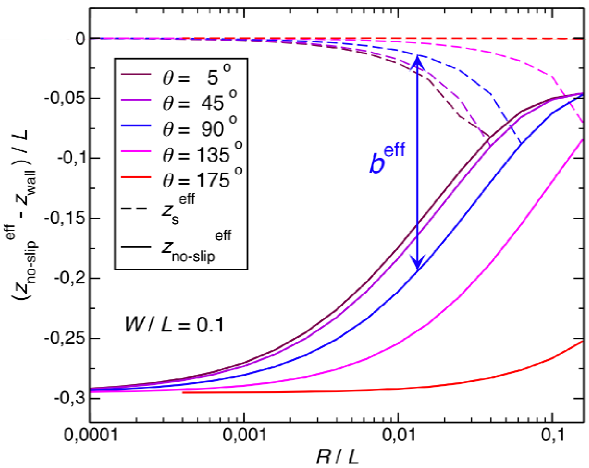

Figure 14: Finite element modeling of the dynamics of a liquid at a SO surface: Evolution of the extrapolated no-slip plane position $z_{\text{no-slip}}^{\text{eff}} = z_s^{\text{eff}} - b^{\text{eff}}$, where z_s^{eff} is the effective shear plane position and b^{eff} the effective slip length, with the radius R of the re-entrant structure (see Fig 5.c), for various Young contact angles; the reference position z_{wall} is chosen to be the top of the pattern (see Fig 5.c).

We investigated the influence of the 're-entrant' curvature on the slip properties, for various Young contact angles. On Fig 14, we plotted the results in terms of extrapolated no-slip plane position inside the walls $z_{\text{no-slip}}^{\text{eff}} = z_s^{\text{eff}} - b^{\text{eff}}$. When the radius R of the re-entrant structure is increased (see Fig 5.c for the definition of R), the slip length $b^{\text{eff}} = z_s^{\text{eff}} - z_{\text{no-slip}}^{\text{eff}}$ starts by diminishing progressively to zero, while the shear plane position z_s^{eff} roughly follows the position of the liquid/vapor meniscus. When the radius R becomes very large, one can observe an effective no-slip BC (with $b^{\text{eff}} = 0$, *i.e.* $z_s^{\text{eff}} = z_{\text{no-slip}}^{\text{eff}}$), and z_s^{eff} goes back toward the top of the pattern. On the whole, one can note that the slip properties can be affected significantly for wetting liquids, as soon as the radius R of the 're-entrant' structure is larger than typically one hundredth of the pattern periodicity L. It is therefore crucial to use an extremely sharp 're-entrant' structure (with $R/L < 0.01$) if one wants oil to slip efficiently on SO surfaces.

B Dissipation around a SO surface

In this appendix we will focus on the dissipation in the system considered in section 4: a liquid is confined between a smooth wall and a ridged SO surface (see Fig 12), and a Couette flow perpendicular to the ridges is imposed by moving the upper (smooth) wall at constant velocity, while maintaining the lower (SO) wall at rest.

We plotted in Fig 15 the local dissipation in the system for different values of the Young contact angle ($\cos\theta$ = -0.5, 0.5 and 0.6). We showed both the local viscous dissipation [$\eta/2(\partial_x v_x + \partial_z v_z)^2$] and the local dissipation due to the walls [$\boldsymbol{f}_{\text{wall}} \cdot \boldsymbol{v}$]. The dissipation is normalized in all cases by the expected dissipation for a homogeneous shear flow: $\eta\gamma^2$, where γ is the average shear rate measured in the steady state. The viscous dissipation inside the liquid is thus expected to be around the unity, while the contribution of the walls is expected to increase linearly with the bare slip length b^0, if we consider the macroscopic situation of a planar wall using the Navier BC. Indeed, the surface dissipation is given by λv_s^2, where λ is the friction coefficient related to the slip length by $\lambda = \eta/b^0$, and v_s is the slip velocity, related to b^0 and γ through the Navier BC: $v_s = b^0\gamma$. The surface dissipation due to the walls is thus $\eta\,\gamma^2\,b^0$ in the macroscopic approach.

In our method however, friction with the wall is modeled by a volume friction in a narrow region of thickness σ from the wall, so as to account for the atomic corrugation (σ is an atomic length). The quantity plotted in Fig 15 is thus a local volume dissipation, and not a surface dissipation. To make the connection with the macroscopic formula, we must define a dissipation density in the vicinity of the wall by spreading the surface dissipation over a thin layer of thickness σ. We can thus expect our measurements to be proportional to $\eta\,\gamma^2\,b^0/\sigma$. The prefactor is not known analytically, and is expected to depend on the details of the model, but we can check the b dependence quantitatively. For $\cos\theta$ = -0.5 the bare slip length of the wall is b^0 = 11.4 nm and the maximum value of the dissipation close to the top planar wall is $d_{\max}$ = 25 $\eta\gamma^2$; $\cos\theta$ = 0.5 corresponds to b^0 = 2.73 nm and $d_{\max}$ = 6 $\eta\gamma^2$; and finally $\cos\theta$ = 0.6 to b^0 = 2.49 nm and $d_{\max}$ = 5 $\eta\gamma^2$. We can easily check that the ratio $d_{\max}/b^0$ is almost constant in the three cases (2.19 for $\cos\theta$ = -0.5 and $\cos\theta$ = 0.5, and 2.09 for $\cos\theta$ = 0.6). This dependence in the slip length shows that close to the wall, the local energy dissipation is dominated by the friction with the wall at the molecular scale in non-wetting situations.

To analyze the viscous dissipation, we plotted in Fig 16 the viscous contribution alone. One can see that the maximum value of the dissipation comes from the curved sections of the surface that are oriented at 45° from the shear direction. This is not a surprise since a shear flow can be separated into two components: a rotational flow that does not dissipate energy, and an elongation flow with the main axis precisely oriented at 45° from the shear direction. The elongational component is the only one participating in the dissipation, and one thus observes a maximum in the regions where this component is maximal.

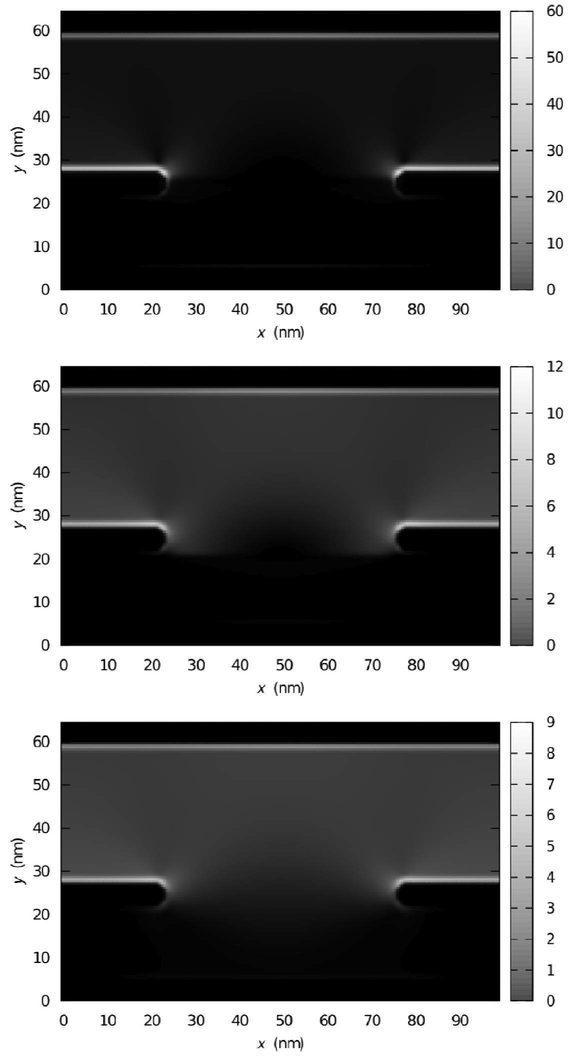

Figure 15: Dissipation inside the fluid and at the walls, in units of $\eta\gamma^2$, where γ is the average shear rate, for $\cos\theta$ = -0.5 (top figure), 0.5 (central figure) and 0.6 (bottom figure).

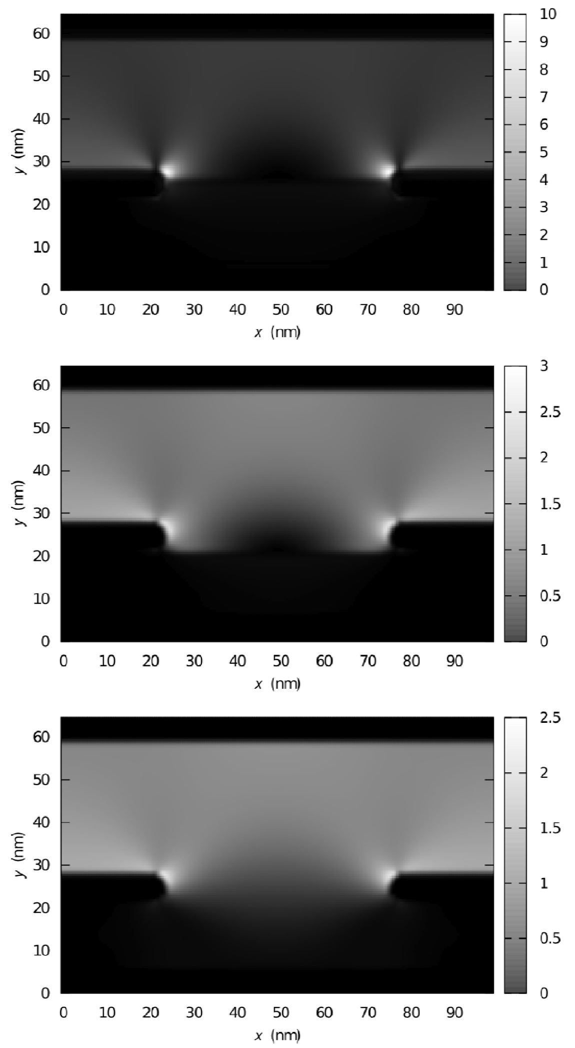

Figure 16: Viscous dissipation alone, in units of $\eta\gamma^2$, where γ is the average shear rate, for $\cos\theta$ = -0.5 (top figure), 0.5 (central figure) and 0.6 (bottom figure).